

SCIENTIFIC REPORTS

OPEN

Synthesis of Vertically Standing MoS₂ Triangles on SiC

Feifei Lan, Zhanping Lai, Yongkuan Xu, Hongjuan Cheng, Zaien Wang, Chengjun Qi, Jianli Chen & Song Zhang

Received: 03 June 2016

Accepted: 25 July 2016

Published: 23 August 2016

Layered material MoS₂ has been attracting much attention due to its excellent electronic properties and catalytic property. Here we report the synthesis of vertically standing MoS₂ triangles on silicon carbon (SiC), through a rapid sulfidation process. Such edge-terminated films are metastable structures of MoS₂, which may find applications in FinFETs and catalytic reactions. We have confirmed the catalytic property in a hydrogen evolution reaction (HER). The Tafel slope is about 54 mV/decade.

In the past few years, transition metal dichalcogenides (TMD) have attracted great attention for their considerable potential applications in the fields of catalysis, microelectronics, optoelectronic devices on both conventional and flexible substrates^{1–9}. Lots of efforts have been made to realize the applications of TMD. But almost all of these works that have been done are based on the platelet-like morphology on the surface of different substrates. In contrast, a few works have been done to use the edges of these layered materials. In fact, vertically standing TMD materials hold high aspect ratio and dangling bonds¹⁰. For MoS₂, the exposed edges means the S dangling bonds. It is the active sites for catalytic reactions. As a layered material, MoS₂ usually expose the basal planes (it means the flat triangles with the Mo atom terminating surface) as the terminating surface with minimal roughness and dangling bonds. But in the condition of vertically standing MoS₂, the edges sites were exposed maximally. The exposed edges with high chemical active and may play an important role in many catalytic reactions, such as hydrogen production^{11–15}, photocatalysis¹⁶, hydrogen evolution reaction (HER), hydrodesulfurization catalyst used for removing sulfur compounds from oil^{17–23}. In addition, these vertical structures of TMD are ideal channel materials for FinFET²⁴. However, edges are usually the rare surface sites of layered materials due to their inherently high surface energy. Increasing the edge dimension is therefore challenging.

Methods

In this work, we develop a rapid sulfidation process through a large carrier gas flow rate on SiC using a CVD method. The MoS₂ triangles are aligned vertically to the surface of the substrate. Various characterizations techniques were used to have a good understand to the mechanism of the vertically standing triangles. Furthermore, HER performance of vertically standing MoS₂ triangles was researched.

The synthesis process of vertically standing MoS₂ triangles is schematically illustrated in Fig. 1. At the beginning, MoO₃ powder was placed in the centre of the furnace, 6H SiC was placed next to the MoO₃ powder. Sulphur powder was placed inside of a steel cylinder out side of the furnace, with a heating tape around it. High pure argon was chosen as carrier gas to convey sulphur and MoO₃ vapor to downstream. The temperature of MoO₃ powder was 1000 °C, sulphur powder was heated to 260 °C, the growth pressure was atmospheric.

A typical optical image of the MoS₂ triangles grown on SiC substrate is shown in Fig. 2a. It clearly shows that most of the triangles on the surface were vertically standing, there are a few flat triangles on the surface. The SEM image demonstrates that the as grown triangles are nearly perpendicular to the substrate. There is a small angles of inclination of some triangles. The edges of different MoS₂ triangles could be clearly observed in SEM images. The lateral dimensions of the triangles are tens micrometer, the heights are from 30 nm to 2 μm. Figure 2c is the Raman spectrum of the vertically standing triangles on SiC and monolayer MoS₂ on sapphire. Two Raman characteristic bands of vertically standing triangles at 410 cm⁻¹ and 383 cm⁻¹ corresponding to A_g¹ and E_{2g}¹ respectively^{25–27}. Comparing to the flat monolayer MoS₂ on sapphire, the intensity ratio between A_g¹ and E_{2g}¹ of the vertically standing triangles is higher, revealing a higher density of exposed edges in those vertically standing triangles. Figure 2d,e are the XPS spectra of Mo 3d and S 2p peak. The Mo 3d shows two peaks at 232.5 eV and 229.2 eV. The peaks, corresponding to the S 2p_{1/2} and S 2p_{3/2} orbital of divalent sulfide ions (S²⁻), are observed at 163.3 and 162 eV. These results agree well with the reported values for MoS₂ crystal^{23,28,29}.

Electronic Material Research Institute of Tianjin, Tianjin 300220, P. R. China. Correspondence and requests for materials should be addressed to F.L. (email: lanfeifei0601@126.com)

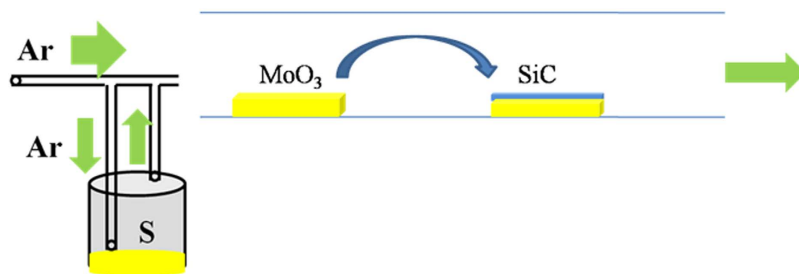


Figure 1. Schematic illustration of the synthesis of vertically standing triangles on SiC.

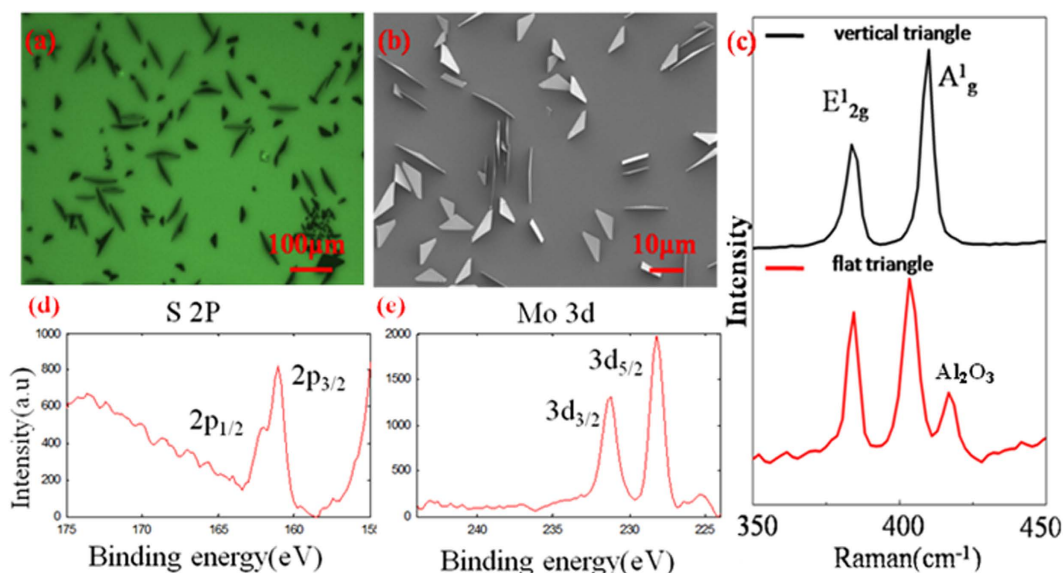


Figure 2. Characterization of synthesized vertically standing MoS₂ triangles. (a) optical image of vertically standing triangles. (b) SEM image to clearly shows the vertically standing triangles. (c) Raman spectrum of the triangles on SiC and single-layer MoS₂ obtained by CVD on sapphire. (d) XPS spectra of Mo 3d. (e) XPS spectra of S 2p peak.

Due to the anisotropic bonding and the general tendency to minimize the surface energy, nanoparticles of layer materials usually exhibit platelet-like morphology^{30,31}. Alternatively, vertically standing triangles can also be obtained by a fast growth process³², the synthesis rate is mainly affected by the diffusion of product gas on the surface of the substrate. By controlling the reactant concentration, we can obtain the MoS₂ films with different morphologies. Through regulating the carrier gas flow rate, the sulfidation rate of MoO₃ can be controlled well. In addition, by changing the carrier gas flow rate, we can have a good understand of the growth process of MoS₂ film.

As shown in Fig. 3a, when the carrier gas flow rate is 100sccm, the concentration of sulfidation vapor is too low to meet the needs. Meanwhile, with a slow carrier gas flow rate, the forming of MoO_{3-x} is limited, and the transport rate of MoO_{3-x} to the surface of substrate is also affected. In this condition, there are only some nanoparticles and some small rectangles on the surface of SiC, because of the lacking of S. So we increasing the carrier gas flow rate to 180sccm, the size of the rectangles increased, but we still do not obtained the vertically standing triangles. When the carrier gas flow increased to 260sccm, the synthesis rate is faster with the increasing of sulfidation concentration. Under this condition, we obtained the vertically standing triangles on the surface of SiC, the result is shown in Fig. 3c. Some of flat triangles were observed on the surface of SiC, only a few vertically standing triangles were obtained. So we increased the carrier gas flow to 340sccm, almost all of the triangles are perpendicular to the substrate, as shown in Fig. 3d. Figure 3e,f were the SEM images of flat rectangles and triangles. Figure 3f–h show the SEM images of vertically standing triangles. From the results, we can see that, only under a fast growth rate, can we get the vertically standing triangles of MoS₂.

To have a better understand, the growth model is shown in Fig. 4. At the beginning of the growth, there was neither buffer layer nor seed on the surface of the substrate, so nucleation process was a 3D. The triangles are all coming from the islands of Fig. 4a. When the carrier gas flow rate is small, the atoms and molecules have enough time to mobility and diffusion on the surface of the substrate, so the synthesis process of MoS₂ will be a 2D growth. With the supply of the sulfur vapor, the small islands grew into larger domain size, at last, the flat triangles of MoS₂ were obtained, as shown in Fig. 4b. When the carrier gas flow rate is high enough, the chemical

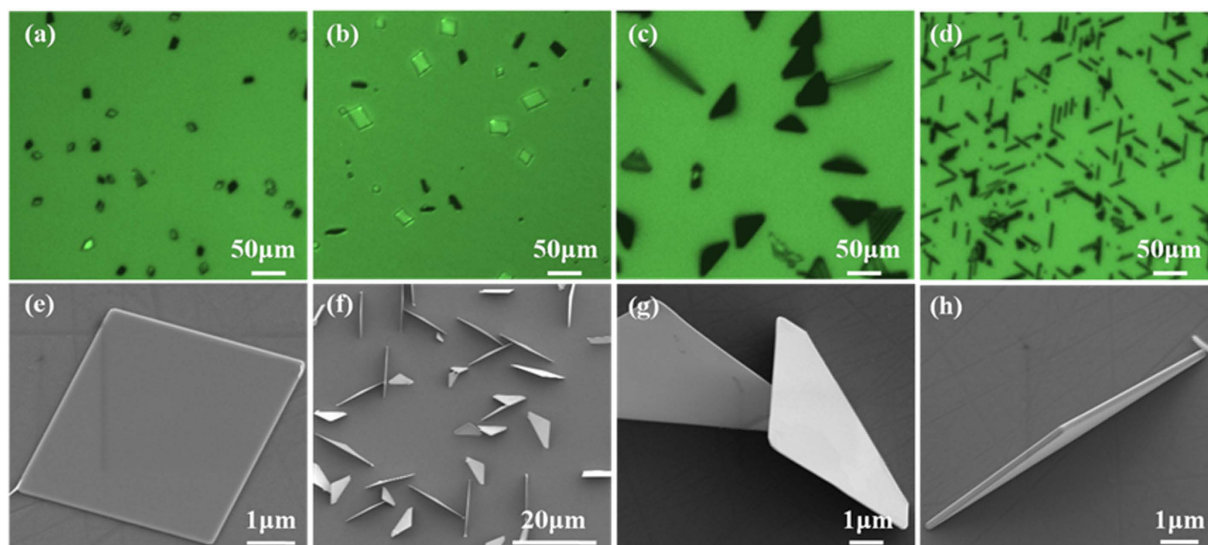


Figure 3. Optical and SEM images of MoS₂ triangles. (a–d) optical images of the MoS₂ triangles with different carrier gas flow rates. (e) SEM image of MoS₂ rectangles with a low condition of sulfur. (f–h) SEM images of vertically standing MoS₂ triangles.

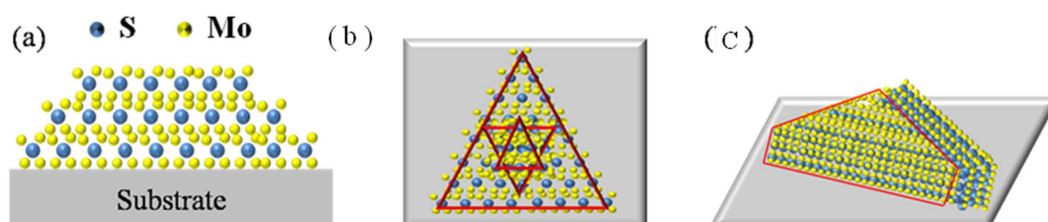


Figure 4. Growth model of vertically standing and flat MoS₂ triangles.

conversion occurs much faster than the diffusion of sulfur gas into the film. Under this condition, the sulfidation process will be rate-limiting. Meanwhile, with the anisotropic structure, the diffusion along the layers through van der Waals gaps is much faster than diffusion across the layers. Accordingly, the layers naturally orient perpendicular to the film, exposing van der Waals gaps for fast reaction. In this condition, the vertically structure formed, as shown in Fig. 4c.

As we know, the wettability has a great effect to the nucleation process at the beginning of the growth. If the wettability of the substrate is good, the film will be a two dimensional growth, along the surface of the substrate, then flat film will be obtained. If the wettability of the substrate is poor, the film will maintain a 3D growth along the layers. In order to prove our conclusion, and have a contrast, we also synthesis the MoS₂ film on sapphire with the same condition: the temperature of MoO₃ powder is 1000 °C, carrier gas flow rate were 100sccm, 180sccm, 260sccm, 340sccm respectively. The results were shown in Fig. 5. we can see that, the film on the sapphire are all flat triangles. There is no vertically standing triangles obtained on the sapphire. This is because the perfect wettability of MoS₂ on the sapphire, the growth process will be 2D. Under this condition, there will not be vertically standing triangles formed. In contrast, with a poor wettability between MoS₂ and SiC, the nucleation of the film on the surface of SiC is more difficult, and the growth process will be 3D, which is useful to synthesis the vertically standing triangles. Through the results, we can see that the wettability is also a important factor during the growth of the vertically standing MoS₂.

HER catalytic activity of vertically standing MoS₂ triangles on SiC was tested. Typical cathodic polarization curves and corresponding Tafel plots are shown in Fig. 6a,b. The Tafel slope in our vertically standing triangles was about 54 mV/decade. The related reports about vertically standing structures of MoS₂ is about 94 mV/dec¹⁰ and 105–120 mV/dec²³. Tafel plots are commonly used to evaluate the efficiency of the catalytic reaction, which indicated that the surface coverage of absorbed hydrogen was relatively low. The small Tafel plots means the high efficiency of the reaction. This indicating a good catalytic property of vertically standing triangles on SiC.

Conclusions

We have developed a rapid sulfidation process for the synthesis of vertically standing MoS₂ triangles. SEM images reveal the synthesis mechanism of the triangles. It is suggested that under a high concentration of sulfur, the growth process will by a 3D growth, all these vertically standing triangles come from the small islands on the surface of SiC. In addition, by a comparison between the films grown on sapphire and SiC, we find the wettability

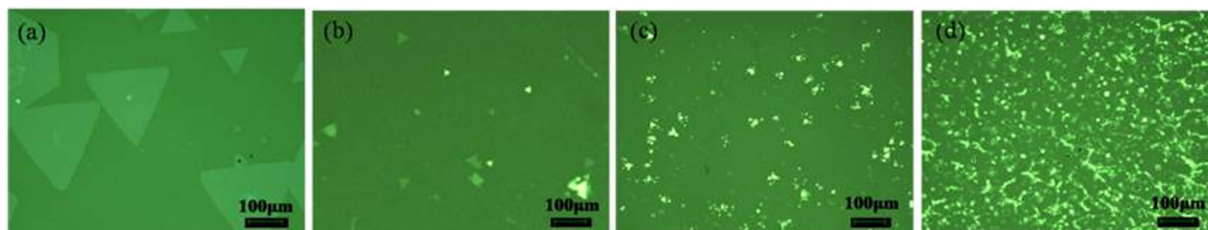


Figure 5. Optical microscope images of the synthesis MoS₂ on Al₂O₃ with the carrier gas flow rate of 100sccm, 180sccm, 260sccm, 340sccm.

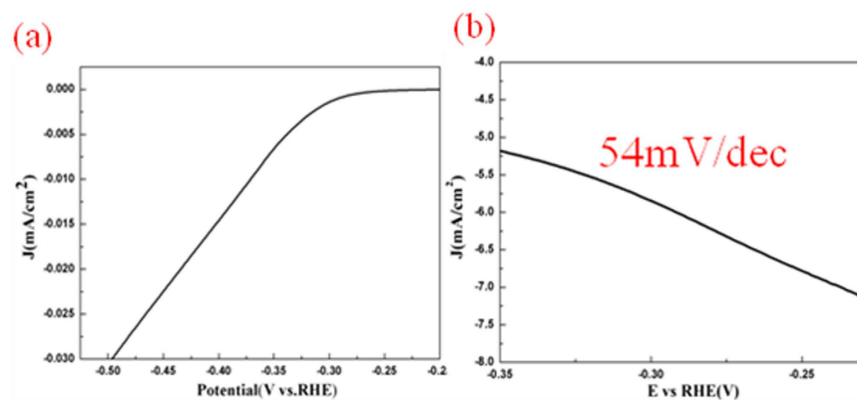


Figure 6. Cathodic polarization curves of vertically standing triangles, Tafel plots of vertically standing triangles.

is another factor for the forming of vertically standing triangles. At last, the HER properties of the triangles was tested. The Tafel slope is about 54 mV/decade, which is much smaller than the related reports about vertically standing MoS₂ nanosheets.

References

1. R. Tenne, L. Margulis, M. Genut & G. Hodes. Polyhedral & cylindrical structures of tungsten disulphide. *Nature* **360**, 444–446 (1992).
2. Y. Feldman, E. Wasserman, D. J. Srolovitz & R. Tenne. High-Rate, Gas-Phase Growth of MoS₂ Nested Inorganic Fullerenes & Nanotubes. *Science* **267**, 222–225 (1995).
3. Y. Golan *et al.* Microtribology & Direct Force Measurement of WS₂ Nested Fullerene-Like Nanostructures. *Adv. Mater* **11**, 934–937 (1999).
4. J. Huang, S. Somu & A. Busnaina. A molybdenum disulfide/carbon nanotube heterogeneous complementary inverter. *Nanotechnology* **23**, 5203–5208 (2012).
5. Y. Zhang, J. Ye, Y. Matsushashi & Y. Iwasa. Ambipolar MoS₂ thin flake transistors. *Nano Lett* **12**, 1136–1140 (2012).
6. H. Liu, A. T. Neal & Peide D. Ye. Channel length scaling of MoS₂ MOSFETs. *ACS NANO* **6**, 8563–8569 (2012).
7. Edney, G. S. Firmiano *et al.* Graphene oxide as a highly selective substrate to synthesize a layered MoS₂ hybrid electrocatalyst. *Chem. Commun* **48**, 7687–7689 (2012).
8. B. Hinnemann *et al.* Biomimetic hydrogen evolution: MoS₂ nanoparticles as catalyst for hydrogen evolution. *J. Am. Chem. Soc* **127**, 5308–5309 (2005).
9. T. F. Jaramillo *et al.* Identification of active edge sites for electrochemical H₂ evolution from MoS₂ nanocatalysts. *Science* **317**, 100–102 (2007).
10. D. Kong *et al.* Synthesis of MoS₂ and MoSe₂ films with vertically aligned layers. *Nano Lett* **13**, 1341–1347 (2013).
11. T. F. J. *et al.* Identification of active edge sites for electrochemical H₂ evolution from MoS₂ nanocatalysts. *Science* **317**, 100–102 (2007).
12. B. H. *et al.* Biomimetic hydrogen evolution: MoS₂ nanoparticles as catalyst for hydrogen evolution. *J. Am. Chem. Soc.* **127**, 5308–5309 (2005).
13. D. Kong *et al.* Synthesis of MoS₂ and MoSe₂ films with vertically aligned layers. *Nano Lett.* **13**, 1341–1347 (2013).
14. H. I. Karunadasa *et al.* A molecular MoS₂ edge site mimic for catalytic hydrogen generation. *Science* **335**, 698–702 (2012).
15. D. Merki, S. Fierro & X. Hu. Fe, Co, and Ni ions promote the catalytic activity of amorphous molybdenum sulfide films for hydrogen evolution. *Chem. Sci.* **3**, 2515–2525 (2012).
16. J. Wilcoxon, T. Thurston & J. Martin. Applications of metal and semiconductor nanoclusters as thermal and photo-catalysts. *Nanostruct Mater* **12**, 993–997 (1999).
17. J. Lauritsen *et al.* Atomic-scale structure of Co–Mo–S nanoclusters in hydrotreating catalysts. *J. Catal* **197**, 1–5 (2001).
18. T. Todorova, R. Prins & T. Weber. A density functional theory study of the hydrogenolysis and elimination reactions of C₂H₅SH on the catalytically active (100) edge of 2H-MoS₂. *J. Catal* **246**, 109–117 (2007).
19. P. G. Moses, B. Hinnemann, H. Topsøe & J. K. Nørskov. The hydrogenation and direct desulfurization reaction pathway in thiophene hydrodesulfurization over MoS₂ catalysts at realistic conditions: a density functional study. *J. Catal* **248**, 188–203 (2007).

20. J. V. Lauritsen *et al.* Location and coordination of promoter atoms in Co- and Ni-promoted MoS₂-based hydrotreating catalysts. *J. Catal* **249**, 220–233 (2007).
21. P. Raybaud *et al.* Ab initio study of the H₂–H₂S/MoS₂ gas–solid interface: The nature of the catalytically active sites. *J. Catal* **189**, 129–146 (2000).
22. J. Lauritsen *et al.* Atomic-scale insight into structure and morphology changes of MoS₂ nanoclusters in hydrotreating catalysts. *J. Catal* **221**, 510–522 (2004).
23. H. Li, H. Wu, Sh Yuan & He Qian. Synthesis and characterization of vertically standing MoS₂ nanosheets. *Sci. Rep.* **6**, 2117–2124 (2016).
24. M. Chen *et al.* TMD FinFET with 4 nm thin body and back gate control for future low power technology. *IEEE*. **978**, 4673–9894 (2015).
25. Bret, C. Windom, W. G. Sawyer & David, W. Hahn. A Raman spectroscopic study of MoS₂ and MoO₃: applications to tribological systems. *Tribol Lett.* **42**, 301–310 (2011).
26. H. Li *et al.* From bulk to monolayer MoS₂: evolution of Raman scattering. *Adv. Funct. Mater* **22**, 1385–1390 (2012).
27. B. Chakraborty, H. S. S. R. Matte, A. K. Sood & C. N. R. Rao. Layer-dependent resonant Raman scattering of a few layer MoS₂. *Raman Spectrosc.* **44**, 92–96 (2013).
28. K. Lee *et al.* Electrical Characteristics of Molybdenum Disulfide Flakes Produced by Liquid Exfoliation. *Adv. Mater.* **23**, 4178–4182 (2011).
29. Zh Lu *et al.* *In situ* fabrication of porous MoS₂ thin-films as high-performance catalysts for electrochemical hydrogen evolution. *Chemical Communication.* **10**, 1039–1042 (2013).
30. D. Kong *et al.* Few-layer nanoplates of Bi₂Se₃ and Bi₂Te₃ with highly tunable chemical potential. *Nano Lett.* **10**, 2245–2250 (2010).
31. Y. Li *et al.* MoS₂ nanoparticles grown on graphene: an advanced catalyst for the hydrogen evolution reaction. *Am. Chem. Soc.* **133**, 7296–7299 (2011).
32. Y. Cheng *et al.* Van der Waals epitaxial growth of MoS₂ on SiO₂/Si by chemical vapor deposition. *RSC Adv.* **3**, 17287–17293 (2013).

Author Contributions

Z.L., Y.X. and H.C. H.J. conceived the experiments. F.L., Z.W. and C.Q. synthesized the MoS₂ flakes. J.C. and S.Z. performed the characterizations of Raman, SEM, optical microscope and HER catalytic activity. F.L. and Y.X. wrote the manuscript. All authors reviewed the manuscript.

Additional Information

Competing financial interests: The authors declare no competing financial interests.

How to cite this article: Lan, F. *et al.* Synthesis of Vertically Standing MoS₂ Triangles on SiC. *Sci. Rep.* **6**, 31980; doi: 10.1038/srep31980 (2016).



This work is licensed under a Creative Commons Attribution 4.0 International License. The images or other third party material in this article are included in the article's Creative Commons license, unless indicated otherwise in the credit line; if the material is not included under the Creative Commons license, users will need to obtain permission from the license holder to reproduce the material. To view a copy of this license, visit <http://creativecommons.org/licenses/by/4.0/>

© The Author(s) 2016